

## **APPENDIX A**

### **FLOW IN THE CALICO HILLS NONWELDED VITRIC UNIT (RESPONSE TO RT 1.01 AND GEN 1.01 (COMMENT 26))**

### **Note Regarding the Status of Supporting Technical Information**

This document was prepared using the most current information available at the time of its development. This Technical Basis Document and its appendices providing Key Technical Issue Agreement responses that were prepared using preliminary or draft information reflect the status of the Yucca Mountain Project's scientific and design bases at the time of submittal. In some cases this involved the use of draft Analysis and Model Reports (AMRs) and other draft references whose contents may change with time. Information that evolves through subsequent revisions of the AMRs and other references will be reflected in the License Application (LA) as the approved analyses of record at the time of LA submittal. Consequently, the Project will not routinely update either this Technical Basis Document or its Key Technical Issue Agreement appendices to reflect changes in the supporting references prior to submittal of the LA.

## **APPENDIX A**

### **FLOW IN THE CALICO HILLS NONWELDED VITRIC UNIT (RESPONSE TO RT 1.01 AND GEN 1.01 (COMMENT 26))**

This appendix provides a response for Key Technical Issue (KTI) agreement entitled Radionuclide Transport (RT) 1.01. This agreement relates to providing additional information on the technical basis for the proportion of fracture flow through the Calico Hills nonwelded (CHn) vitric units.

#### **A.1 KEY TECHNICAL ISSUE AGREEMENT**

##### **A.1.1 RT 1.01 and GEN 1.01 (Comment 26)**

Agreement RT 1.01 was reached during the U.S. Nuclear Regulatory Commission (NRC)/U.S. Department of Energy (DOE) Technical Exchange and Management Meeting on Radionuclide Transport on December 5 to 7, 2000 (Reamer and Williams 2000), in Berkeley, California. RT subissue 1, radionuclide transport through porous rock, was discussed at that meeting.

At that meeting the NRC expressed concern that the C-Wells tests provide an example that suggests a portion of the flow path is not acting as a single-continuum porous medium (Reamer and Gil 2001). Specifically, the NRC staff indicated that although the Calico Hills nonwelded vitric (CHnv) unit was considered a porous medium, due to its matrix permeability that was considered high enough to accommodate the percolation rates expected for Yucca Mountain, the Calico Hills nonwelded zeolitic (CHnz) unit has a matrix permeability that may accommodate only a relatively small portion of the percolation rate, and, consequently, most of the water may bypass the zeolitic unit in fractures. The NRC also stated that it remained to be demonstrated that the Calico Hills nonwelded unit behaves as a single-continuum porous medium. In response, the DOE pointed out that the current models represent flow and transport through all unsaturated zone units using a dual-continuum approach. Most, but not all, of the flow and transport occurs through the matrix of the CHnv unit. In the CHnz, most, but not all, of the flow and transport is through fractures. The DOE agreed to provide the technical basis for the proportion of fracture flow through the CHnv unit.

General agreement (GEN) 1.01 was reached during the NRC/DOE Technical Exchange and Management Meeting on Range of Thermal Operating Temperatures, held September 18 to 19, 2001 (Reamer and Gil 2001). At that meeting, the NRC provided additional comments, resulting in GEN 1.01 (Comment 26), which relates to RT 1.10. The specific section or page number referral cited below as part of GEN 1.01 (Comment 26) is from *FY01 Supplemental Science and Performance Analyses, Volume 1: Scientific Bases and Analyses* (BSC 2001).

The wording of the agreement is as follows:

#### **RT 1.01**

Provide the basis for the proportion of fracture flow through the Calico Hills non-welded vitric. DOE will revise the AMR UZ Flow Models and Submodels

and the AMR Calibrated Properties Model to provide the technical basis for the proportion of fracture flow through the Calico Hills Nonwelded Vitric. These reports will be available to the NRC in FY 2002. In addition, the field data description will be documented in the AMR In Situ Field Testing of Processes in FY 2002.

#### **GEN 1.01 (Comment 26)**

The multiple interacting continuum (MINC) method is asserted to be better than the dual permeability model (DKM) and to produce “relatively conservative results”. This has not been supported in the SSPA, nor does the referenced AMR provide any more detailed comparison of the two numerical approaches. Furthermore, the referenced AMR (*Conceptual and Numerical Models for UZ Flow and Transport*) indicates that “the dual-continuum approach is expected to give conservative predictions of radionuclide transport in the unsaturated zone.”

The matrix saturation levels beneath the repository identified in Subsection 11.3.5 seem to be much lower than those discussed in Subsection 11.3.1 (Compare Figures 11.3.1-6 and 11.3.5-2).

#### **DOE Initial Response to GEN 1.01 (Comment 26):**

It has been found in UZ flow and transport modeling that DKM produces more conservative results in terms of radionuclide travel times to the water table, while MINC provides a more realistic representation of the UZ flow and transport system.

TSPA-SR employed the DKM approach, thus yielding a more conservative estimate of UZ performance. DOE acknowledges the need to reconcile the differences should MINC be chosen as the modeling approach to be used in a potential LA.

This is the initial DOE response to the agreements.

#### **A.1.2 Related Key Technical Issue Agreements**

KTI agreement RT 1.01 and GEN 1.01 (Comment 26) is related to RT 3.02, Total System Performance Assessment and Integration (TSPAI) 3.24, and GEN 1.01 (Comment 106). While RT 3.02, TSPAI 3.24, and GEN 1.01 (Comment 106) concern the general use of geochemical and hydrological data in the calibration and validation of the unsaturated zone flow field for all hydrostratigraphic units below the repository, RT 1.01 and GEN 1.01 (Comment 26) are specifically related to the justification of the approach for modeling flow through the CHnv unit (i.e., dominant matrix flow). Responses to agreements RT 3.02, TSPAI 3.24, and GEN 1.01 (Comment 106) are provided in Appendix B.

## **A.2 RELEVANCE TO REPOSITORY PERFORMANCE**

Flow and transport through the unsaturated zone plays an important part in the assessment of total system performance, as the unsaturated zone is one of the key natural barriers upon which the repository will rely. The CHn unit is a major hydrogeologic unit underneath the repository. Since fractures are the main pathways for radionuclide transport in the CHnv unit (BSC 2003a, Section 6), the determination of the relative flow proportion through fractures of the CHnv is, therefore, important for unsaturated zone transport calculations.

## **A.3 RESPONSE**

KTI agreement RT 1.01 and GEN 1.01 (Comment 26) relate to the documentation and basis for conceptualization and modeling of the CHn vitric units as a single-porosity matrix in the unsaturated zone flow model (BSC 2003b). In the vitric portions of the CHn units, most of the liquid flow occurs in the matrix, whereas in all other CHn layers, liquid flow occurs predominantly in the fractures. The dominance of matrix flow results from relatively high matrix permeabilities and low fracture densities in the CHn nonwelded vitric layers (BSC 2003c, Section 6.1).

Correspondingly, the vitric layers in the CHn units are conceptualized and handled as a single-porosity matrix only in the unsaturated zone flow model. The effect of fractures on flow and transport within Calico Hills vitric zones is considered negligible and is not modeled (BSC 2003b).

The above conceptual model of matrix-only flow in the CHn vitric unit is supported by the small proportion of fracture flow and dominance of matrix flow, which was qualitatively substantiated by field observation results. Field evidence was obtained from the tracer tests in Busted Butte (BSC 2003d, Section 6.13) at the vitric layer in the upper CHn. Observation showed that flow took place in the matrix and that a preferential (fracture) flow did not develop along a fracture present in the area of the developed fluorescein plume (BSC 2003d, Section 6.13). A detailed description of the Busted Butte tracer test is given in Section A.4.3.

Corroborative evidence is found in field testing along a fault at the Exploratory Studies Facility (ESF) Alcove 4 in the Paintbrush nonwelded (PTn) hydrological unit. The PTn unit has properties similar to the CHn vitric units. Both the PTn units and the CHn vitric units have relatively high matrix permeability and low degree of fracturing, with the former having lower matrix permeability and smaller fracture spacing than the latter. The field test at the ESF Alcove 4 also reveals that the PTn unit has a significant dampening effect on fracture flow, because of matrix imbibition of water flowing along the fault (BSC 2003d, Section 6.7). The ESF Alcove 4 test is described in Section A.4.4.

The above field-observation results obtained at the Busted Butte and Alcove 4 tests provide qualitative evidence to support the conceptual model of matrix-only flow in the CHn units.

GEN 1.01 (Comment 26) concerns the use of the multiple interacting continuum (MINC) method modeling approach to be used in the generation of flow fields, as opposed to the dual-permeability method. In fact, the unsaturated zone flow model adopts the dual-continuum approach for flows through both the fractures and matrix (BSC 2003b, Section 6.1.2). Because

the dual-continuum approach produces results on the conservative side, due to faster breakthrough of radionuclides (BSC 2004, Figure 7-9, Section 7.2), the unsaturated zone flow model is considered to have yielded relatively conservative flow fields. The technical basis for this response to the GEN 1.01 comment is given in Section A.4.5. A brief summary of the basis for the KTI responses is given in Section A.4.6. The technical basis for all the above responses is provided in Section A.4.

The information in this report is responsive to agreement RT 1.01 and GEN 1.01 (Comment 26) made between the DOE and the NRC. This report contains the information that the DOE considers necessary for the NRC to review for closure of these agreements.

## **A.4 BASIS FOR THE RESPONSE**

In the unsaturated zone flow model, matrix and fracture flow in the fractured tuffs was modeled using the dual-permeability method. However, the vitric portions in the CHn units were conceptualized and modeled as a single-porosity matrix unit. This approach is supported by the observation from tracer testing at Busted Butte and is substantiated by corroborative results from field testing at the ESF Alcove 4 in PTn units, which have properties similar to the CHn vitric units.

The following is a brief introduction of the dual-permeability model, a description of the vitric layers, and discussion of the relevant results from the Busted Butte tracer test and the ESF Alcove 4 test.

### **A.4.1 Dual-Permeability Modeling Approach**

The dual-permeability modeling approach (also called dual-continuum approach) was chosen here for describing flow and transport in the unsaturated zone. It considers global flow occurring not only between fractures but also between matrix gridblocks, as well as interflow between fractures and matrix. Using this approach, each gridblock of the primary mesh is divided into two connected gridblocks, one for fracture and the other for matrix.

There are alternative modeling approaches, specifically including the discrete fracture-network and MINC approaches. Discrete fracture-network approaches generally involve computational generation of synthetic fracture networks and subsequent modeling of flow and transport in each individual fracture. The MINC model has multiple subgriddings in all the matrix gridblocks to obtain the resolution of the driving pressure, temperature, and mass fraction gradients at the fracture-matrix interface. The concept behind this model is based on the notion that, because of the presence of sinks and sources, changes in fluid pressure, temperature, phase composition, and so on propagate rapidly through the fracture system, but only slowly invade the tight matrix blocks. Therefore, changes in matrix conditions will be controlled locally by the distance from the fractures (Pruess and Narasimhan 1985).

While these alternative approaches have their advantages, both turn out to be too technically impractical or computationally burdensome to be effectively large-scale models for this study. The discrete fracture-network approaches are appealing scientifically and conceptually and technically but impractical for both computation and matching the fracture systems. Similarly, the MINC model may be slightly more accurate in describing fracture-matrix interaction but

computationally challenging. The dual-permeability model is consistently more conservative. This greater conservatism, added to its computationally straight forwardness, lead to the choice of the dual-permeability modeling approach (BSC 2003c, Section 6.1).

#### **A.4.2 Distribution of the Vitric Layers in Calico Hills Nonwelded Tuff Units**

Field observation shows that hydrological properties are heterogeneous in nature at different scales within both the fracture and matrix continua in Yucca Mountain unsaturated zone (e.g., matrix-saturation distributions) (BSC 2003c, Section 6.1). A geologically based, deterministic approach is primarily used for characterizing subsurface heterogeneity in the unsaturated zone (BSC 2003c, Section 6.1). The heterogeneity of hydrological properties is treated as a function of geologic layering, so that any one geologic layer has homogeneous properties (referred to as layer average properties) except where faulting or variable alteration (e.g., zeolitization) is present. In addition, this layering representation of hydrological properties is based on the considerations that (1) the overall behavior of large-scale flow and transport processes are mainly determined by relatively large-scale heterogeneities associated with the geologic structures of the mountain and (2) the heterogeneity model needs to be consistent with the availability of data (BSC 2003c, Section 6.1).

The vitric layers generally have high porosity and permeability and a low degree of fracturing (Table A-1). Portions of the CHn unit and the lower part of the Topopah Spring welded (TSw) unit occur as vitric tuffs below the repository in the UZ model layers tsw39, ch1, ch2, ch3, ch4, ch5, and ch6. They are located in the southwest portion of the model domain (BSC 2003e, Section 6.6.3). This vitric region is complementary to the zeolitized area. Their relation is qualitatively shown in Figure A-1 as an example for the zeolitic and vitric regions in the unsaturated zone model layer ch2. Zeolite data are of a corroborative nature. The low content of zeolite in the lower left region of the figure is not directly interpolated from actual zeolite data points in that area; rather, it comes as a direct extrapolation from several data points to the east (BSC 2003e, Section 6.6.3). The white area within the purple vitric zone corresponds to the Solitario Canyon fault zone. The multiple faults in the fault zone were simplified into a single structural feature (BSC 2003e, Section 5.2, Assumption 7) in the unsaturated zone flow model. The width of the fault zone is on the same scale as the coarse grid spacing in this area. Distribution of the vitric layers in the CHn is plotted in Figures A-2 and A-3.

The vitric and zeolitic regions within the bottom TSw unit and the CHn units are not effectively determined by the absence or presence of zeolite, because of the lack of sufficient zeolite X-ray diffraction data. The boundaries of vitric and zeolitic regions were selected using the results of saturated permeability data (BSC 2003e, Assumption 4), measured rock-property data from boreholes within the unsaturated zone model area (BSC 2003e, Assumption 5), and the location of faults with significant vertical offset (BSC 2003e, Assumption 6, Section 6.6.3). Vitric tuff has a saturated permeability several orders of magnitude greater than that of zeolitic tuff (Table A-1); for both vitric tuff and zeolitic tuff, there is more saturated permeability data available than mineralogic alteration data (e.g., percentage of zeolite). Altered (i.e., zeolitic) nonwelded tuffs have characteristic hydrous secondary minerals, such as zeolites and clays. This fact results in higher estimates of the matrix porosity by the oven-dried method than those by the relative-humidity method, with oven-dried porosities being typically more than 5% higher than relative-humidity porosities. The huge offsets of the CHn layers by major faults (i.e., the Solitario

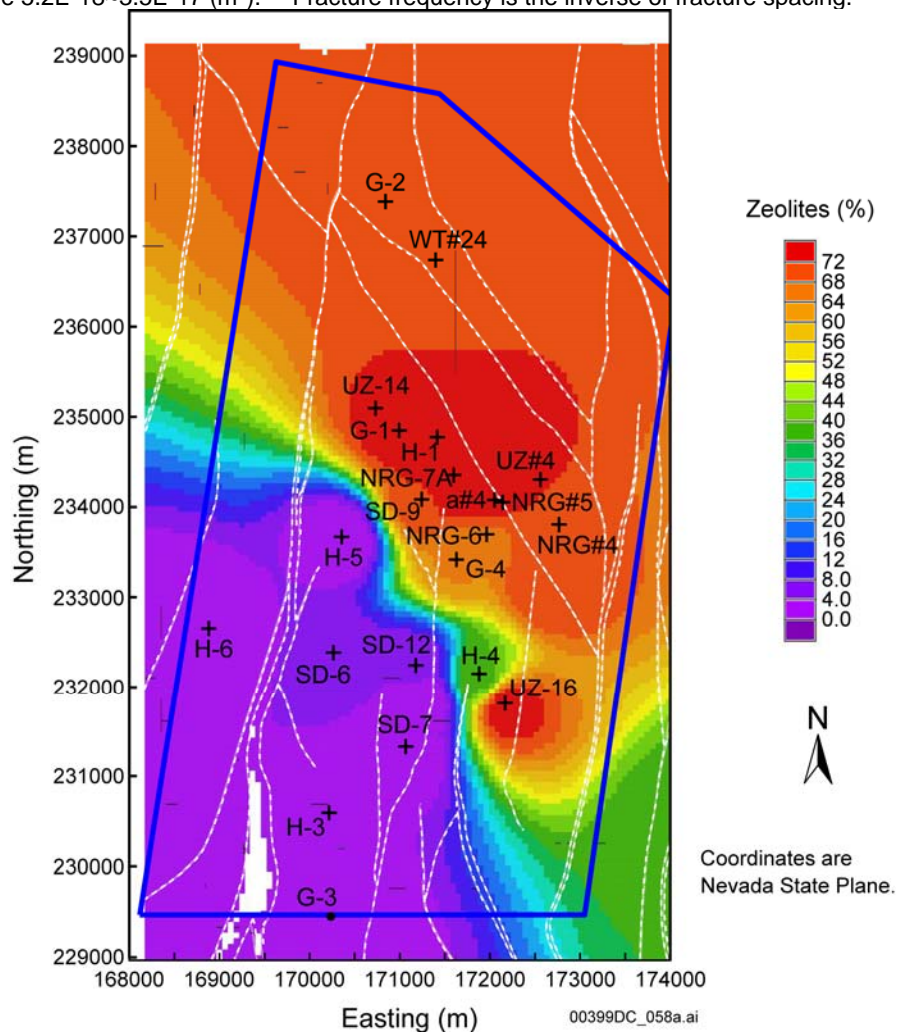
Canyon and Dune Wash faults) have caused enough disparity in elevation and in environment for mineral alteration, with resulting contrasting degrees of zeolitization on different sides of the fault (BSC 2003e, Sections 5.2 and 6.6.3).

Table A-1. Summary of Rock Properties of Selected UZ Model Layers<sup>†</sup>

Units	UZ Model Layers	Porosity	Matrix Permeability (m <sup>2</sup> ) <sup>‡</sup>	Fracture Frequency (m <sup>-1</sup> ) <sup>††</sup>
PTn	ptn21-ptn26 (nonwelded tuff)	0.233~0.498	1.3E-15~6.7E-13	0.46~0.97
TSw	tsw31-tsw38 (welded tuff)	0.043~0.157	2.3E-20~3.2E-16	0.81~4.36
	tsw39 (vitric tuff)	0.229	4.3E-13 <sup>‡</sup>	0.96
CHn	ch1-ch6 (vitric tuff)	0.331~0.346	2.1E-13~1.6E-12 <sup>‡</sup>	0.10~0.14

Source: BSC 2003c, Tables 3, 4, and 6 (modified).

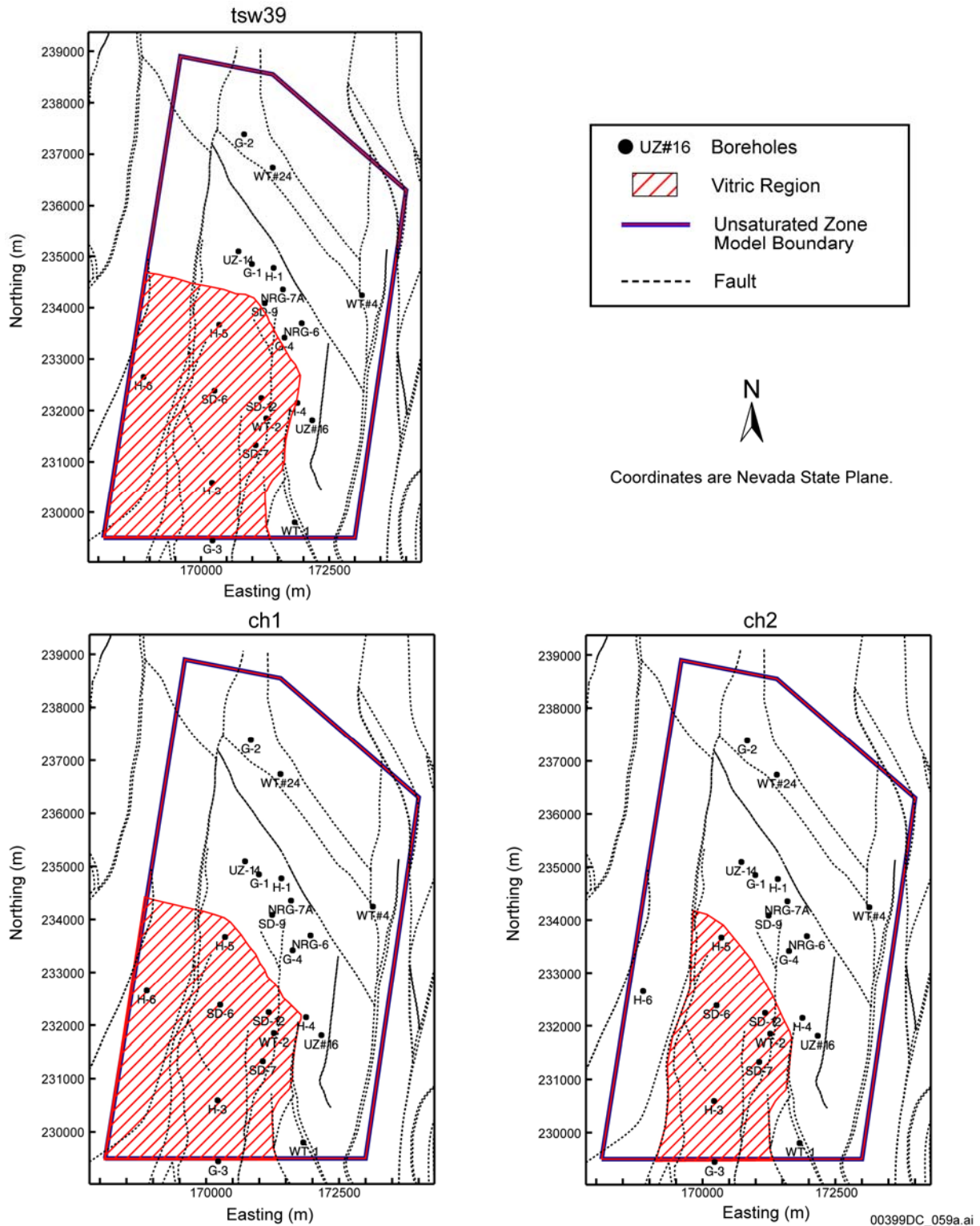
Note: <sup>†</sup>Data are compiled from average value of each UZ model layers. <sup>‡</sup>The layer-averaged permeabilities of all the zeolitic layers are 5.2E-18~3.5E-17 (m<sup>2</sup>). <sup>††</sup>Fracture frequency is the inverse of fracture spacing.



Source: BSC 2003e, Figure 5.

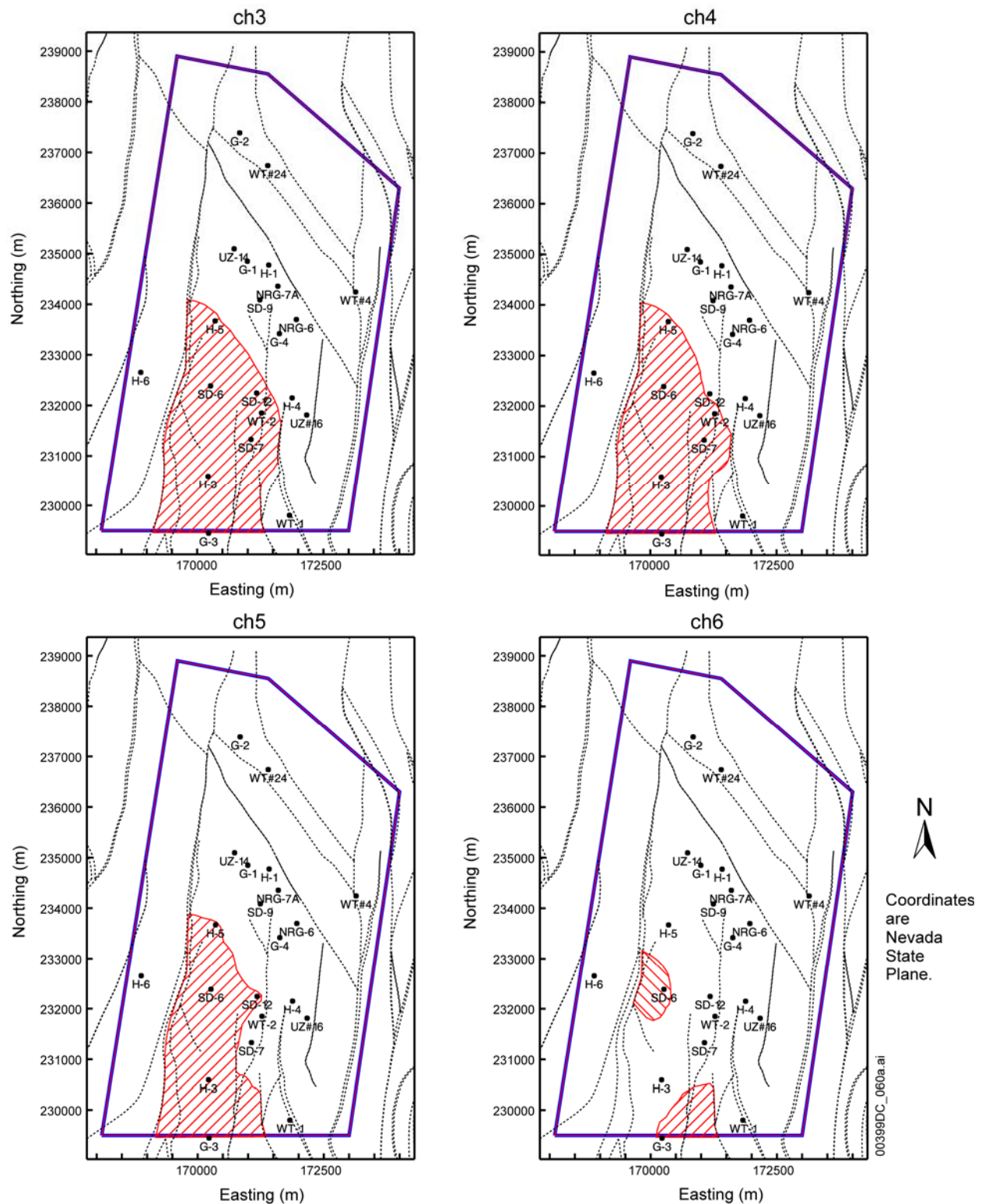
NOTE: The vitric region is denoted by purple. The white area within the purple region corresponds to the Solitario Canyon fault zone. The thick blue line marks the unsaturated zone flow model domain boundary and white dash lines are traces of fault lines.

Figure A-1. Percent Zeolite Distribution of the Unsaturated Zone Model Layer ch2



Source: BSC 2003e, Figure 6a.

Figure A-2. Extent of Vitric Region in Fiscal Year 2002 Unsaturated Zone Model Layers tsw39, ch1, and ch2



Source: BSC 2003e, Figure 6b.

Figure A-3. Extent of Vitric Region in Fiscal Year 2002 Unsaturated Zone Model Layers ch3, ch4, ch5 and ch6

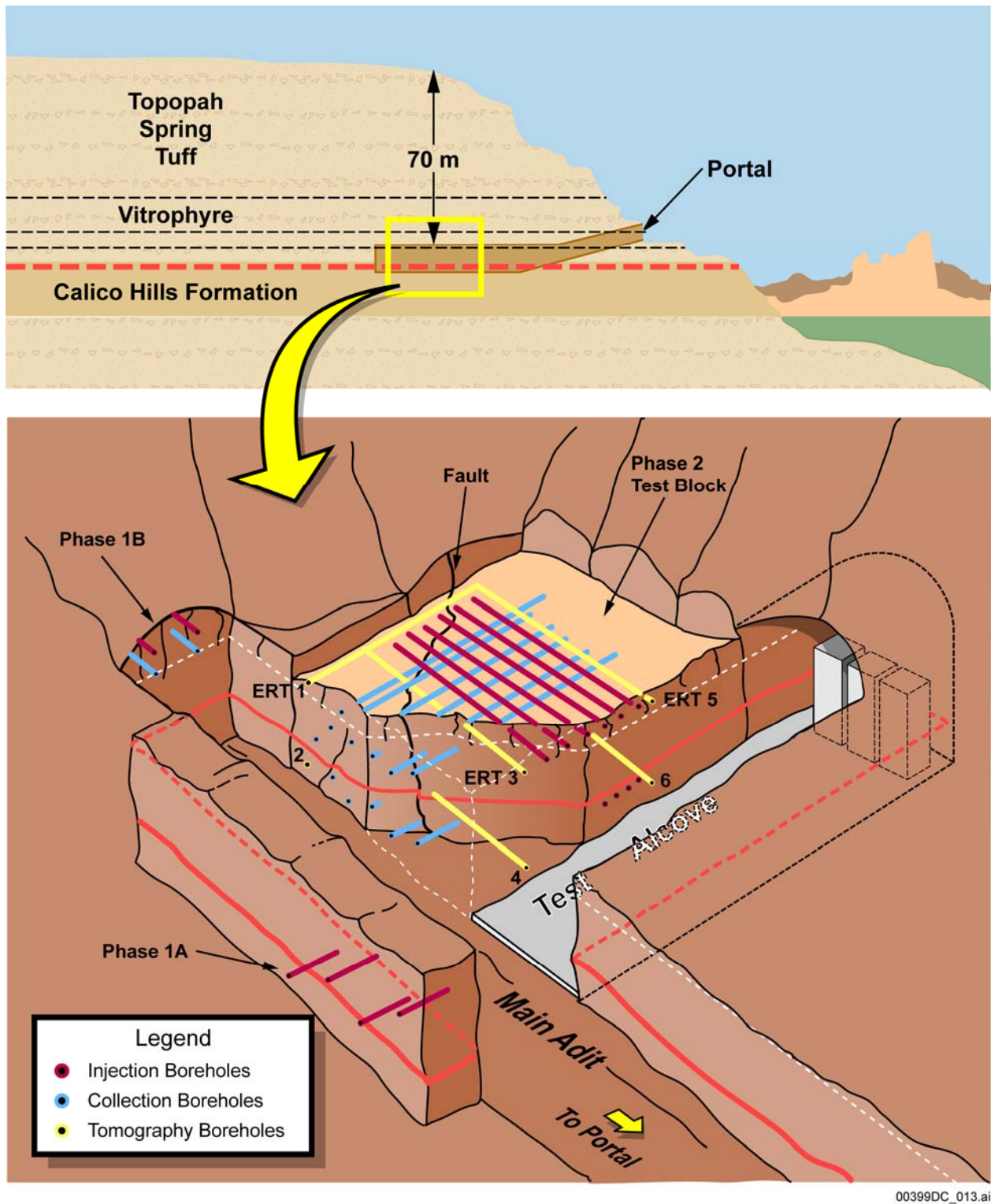
### **A.4.3 Busted Butte Unsaturated Zone Transport Test**

Busted Butte provides a rare exposure of a distal extension of the Calico Hills formation below Yucca Mountain, located 8 km southeast of the repository. The site was chosen based on the presence and similarity of these units to those beneath the repository horizon. The test facility consists of an underground excavation along a lithostratigraphic contact between Topopah Spring tuff (Tpt) and Calico Hills formation (Tac) (i.e., the contact between the TSw and CHn units). Specifically, the contact is made between the nonwelded portion of the basal vitrophyre of Tpt (Tptpv2 (tsw39 (vit)) and Tac (Tptpv1 (ch1 (vit))) (Figure A-4) (BSC 2003b, Table 6.1-1; BSC 2003d, Section 6.13.1.1).

Busted Butte nonwelded vitric layers are exposed around the contact of the Tpt and Tac. These vitric layers have relatively high matrix permeabilities and low fracture densities (Table A-1). The tracer test performed on these vitric layers provides evidence of matrix flow dominance, which is the basis for approximating them as single-porosity matrices.

The principal objectives of the test were to address uncertainties associated with unsaturated zone flow and transport models, including a study of the effect of heterogeneity in unsaturated and partially saturated conditions near the TSw–CHn contact, particularly issues relevant to fracture-matrix interactions and permeability contrast boundaries.

The unsaturated zone transport test site consists of a 75 m long main adit and a 19 m long alcove. The configuration of the unsaturated zone transport test site is shown in Figure A-4.



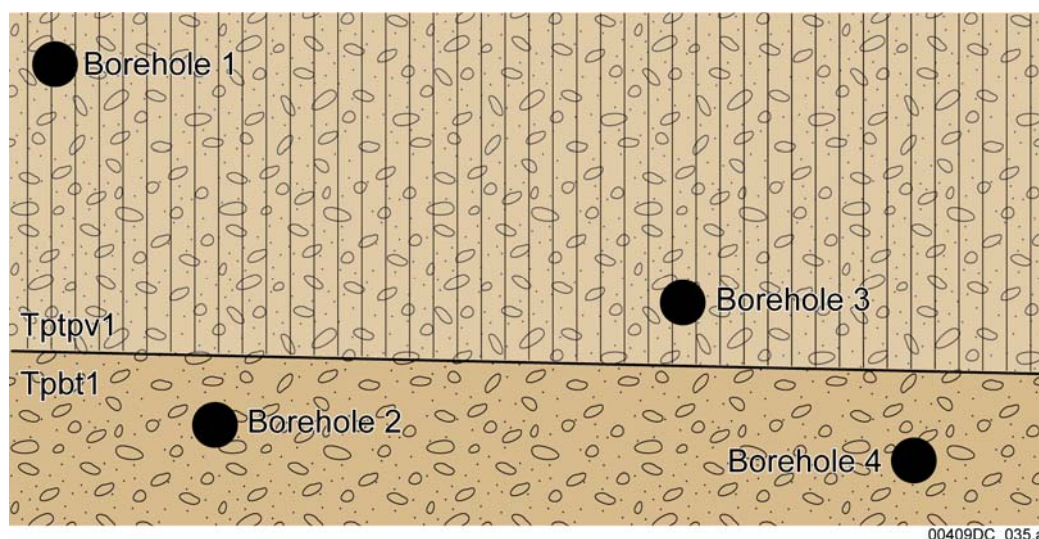
Source: BSC 2003d, Figure 6.13.1-1.

NOTE: This schematic of the Busted Butte unsaturated zone transport test shows the relative locations of the different experiment phases and borehole locations. Schematic is not drawn to scale.

Figure A-4. Busted Butte Unsaturated Zone Transport Test

The unsaturated zone transport test was designed in two test phases. The first phase, including Test Phases 1A and 1B, was designed as a short-term experiment aimed at providing initial transport data on fractures near the contact of the Tpt (TSw) and Tac (CHn), and as a scoping study to assist in design and analysis of Phase 2. The second phase incorporated a larger region than Phase 1, with a broader, more complex scope of tracer injection, monitoring, and collection. Test Phase 1A provides results relevant to KTI RT 1.01 and is discussed here in detail. Other tests are documented in *In Situ Field Testing of Processes* (BSC 2003d, Section 6).

Phase 1A was in Tac (Tptpv1 (chl (vit)) and was a noninstrumented or blind single-point injection test using four boreholes (Figure A-5). Phase 1A used a few tracers, including nonreactive tracers (bromide, fluorescein, pyridone, and fluorinated benzoic acids), a reactive tracer (lithium), and fluorescent polystyrene microspheres (BSC 2003d, Section 6.13.2.1). The tracer of interest is sodium fluorescein, which was used to create images to investigate plume development following the injection. The sodium fluorescein initial concentration was set at  $500 \text{ mg kg}^{-1}$ . An injection rate of 10 mL/hr was applied at boreholes 1 and 3, and a 1 mL/hr rate was applied at boreholes 2 and 4. All the boreholes were 2 m in length and 10 cm in diameter. The injection point was located 90 cm in from the borehole collar. Continuous injection started on April 2, 1998, and ended on January 12, 1999 (286 days).

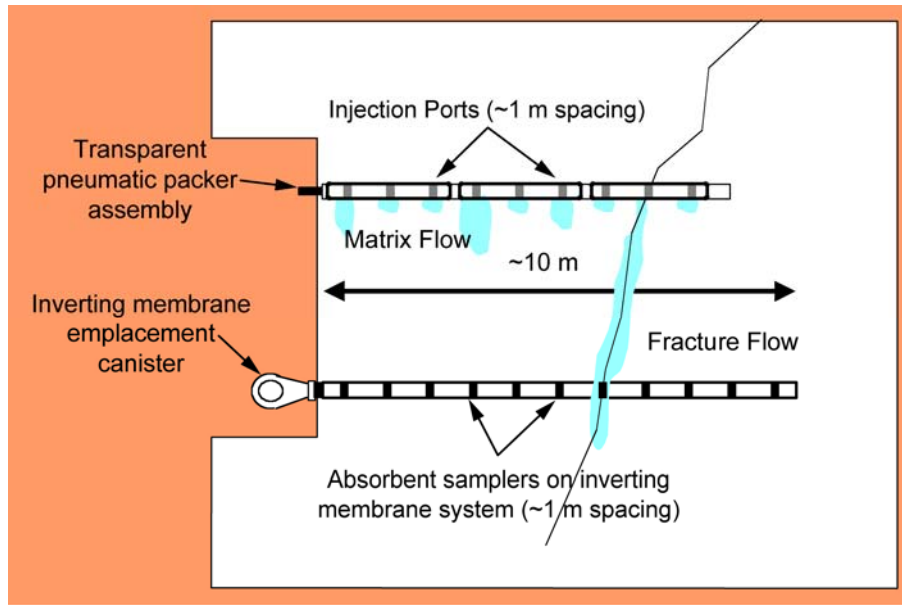


Source: BSC 2003d, Figure 6.13.1-3.

NOTE: Figure not drawn to scale.

Figure A-5. Schematic of Phase 1A Borehole Numbers and Relative Locations

Borehole injection was accomplished by pneumatically inflated borehole sealing and is illustrated in the upper part of Figure A-6. To allow visual inspection of the injection points under both standard and ultraviolet illumination, investigators developed a transparent packer system for the tracer-injection systems (BSC 2003d, Section 6.13.1.6).



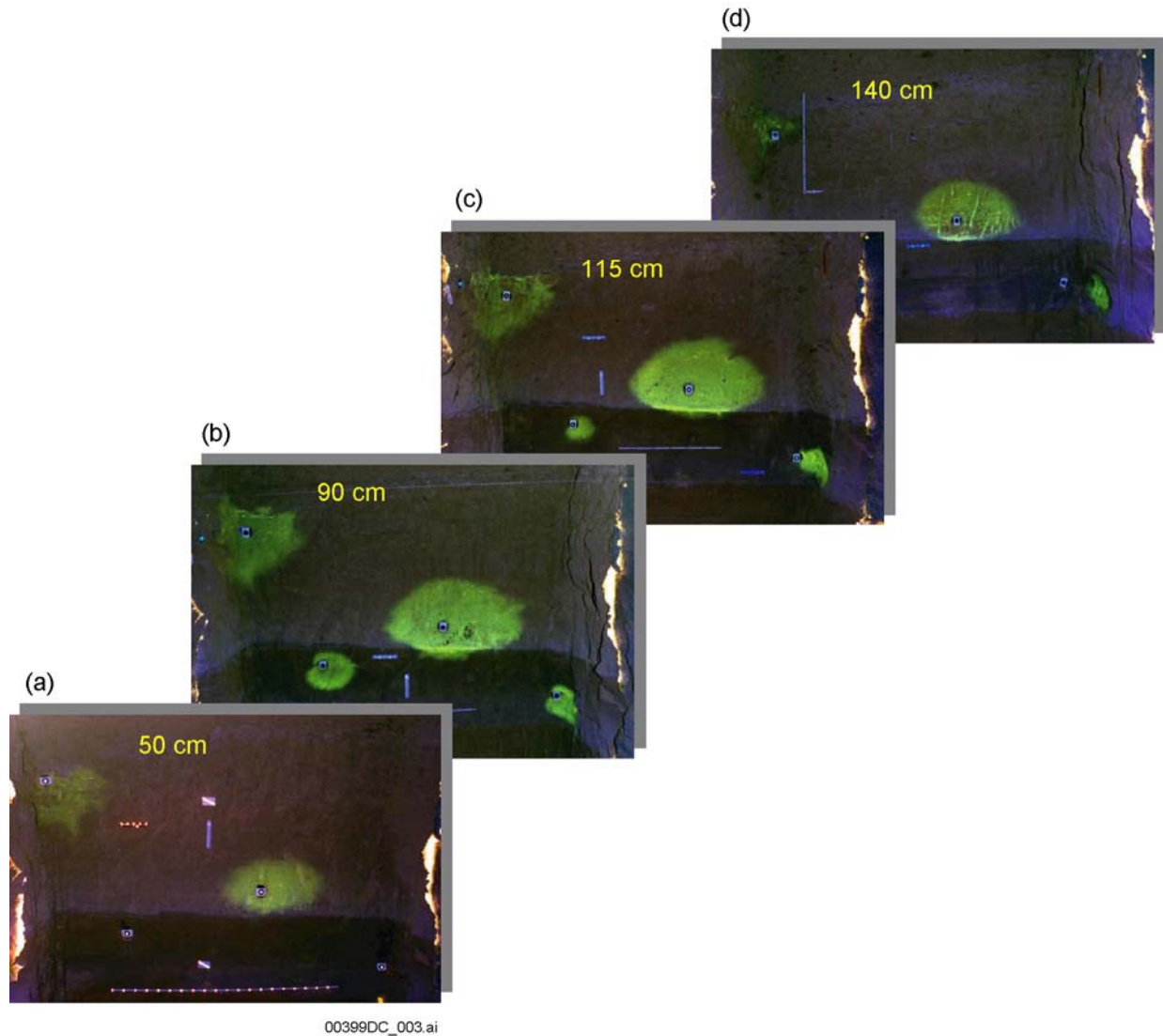
00399DC\_062.ai

Source: BSC 2003d, Figure 6.13.1-2.

NOTE: Injection and collection boreholes are actually perpendicular in plan view. Absorbent sampler spacing is 0.25 to 0.50 m.

Figure A-6. Vertical Cross Section of Injection and Collection System Configuration

Following the injection period, a “mini-mineback” was done to expose the distribution of the tracer in the rock mass. Mineback of the Phase 1A test block began on January 15, 1999, and ended on March 3, 1999. The Phase 1A mineback consisted of four faces exposed at 50, 90, 115, and 140 cm from the adit wall. At each face, the stratigraphy was mapped and surveyed, and images of the fluorescein plume were taken under ultraviolet light. Figure A-7 (a through d) shows the fluorescein plume at each of the mineback faces.



Source: BSC 2003d, Figure 6.13.2-1.

NOTE: The outlines of developing plumes mark the borehole positions identified in Figure A-5.

Figure A-7. Fluorescein Plume at Each of the Four Phase 1A Mineback Faces

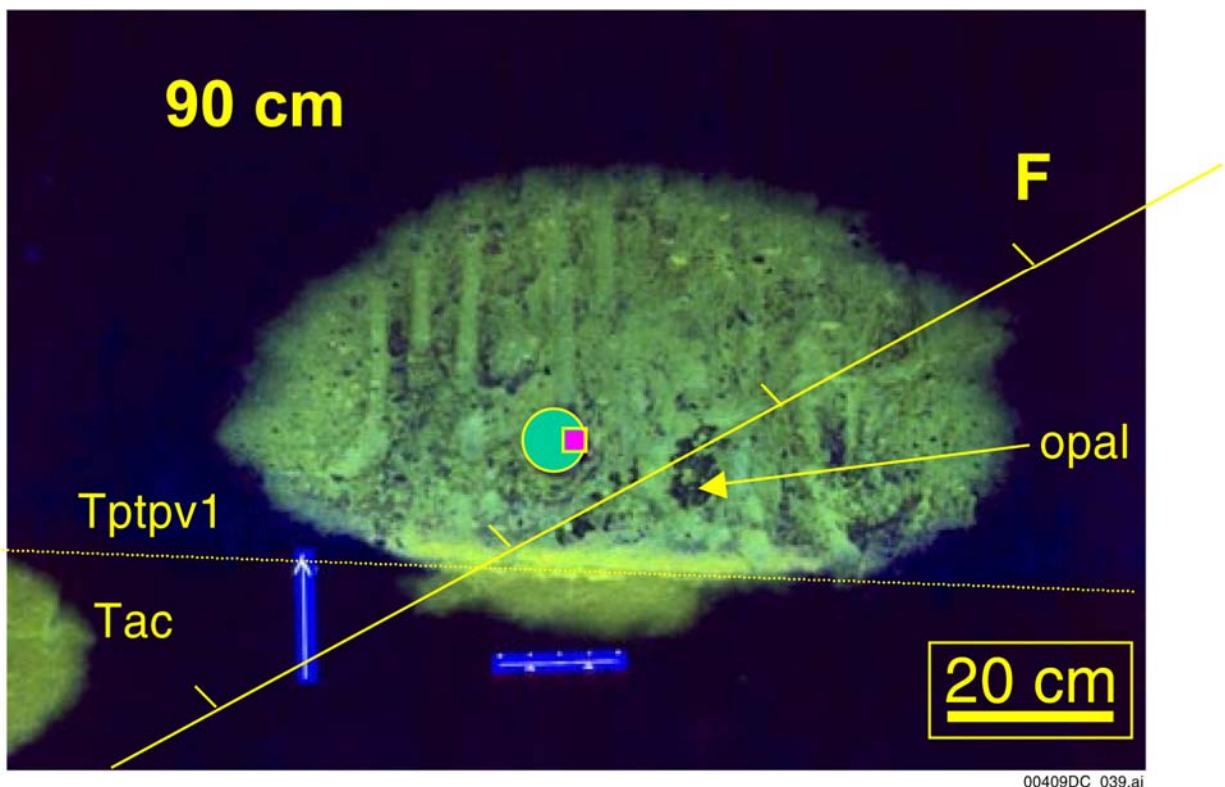
Observations from the Phase 1A test demonstrate strong capillary-dominated flow for both the 1 and 10 mL/hr injection rates. The plumes are relatively uniformly distributed around the injection sites, though some borehole shielding effects (with tracer blocked or delayed from moving in the direction of the borehole) can be seen. Lithologic contacts, however, clearly influence the flow. At all of the mineback faces, the plumes are more oval than round. This reflects the ash layers just above boreholes 2 and 4 and just below borehole 3.

Although difficult to see from the image itself, Figure A-8 shows the location of a small fracture near the injection point in borehole 3. In the upper right edge of the plume, there is a slight perturbation that may have resulted from the presence of the fracture. This indicates that under Phase 1A conditions the fracture is acting as a permeability barrier rather than as a fast path.

There is a slight outburst of the lower part of the plume along the fracture within Tac, which coincides with the contact of the Tptpv1(ch1 (vit)) and Tac. The very short travel along this portion of the fracture can be considered negligible, because the trace does not protrude outside the generally rugged outline of the plume. It may have been caused by the perturbation of the contact surface of the rock layers. Furthermore, preferential flow and transport along this structural discontinuity was not observed. This image demonstrates that fractures have a relatively minor effect on the flow in the Tac (Tptpv1 or ch1 (vit)) units.

Given that the testing was performed under a flow rate much larger than expected under ambient conditions, the effects of fractures in the vitric layers can be considered negligible, and the flow can be reasonably approximated as a single-porosity matrix flow.

This testing result provides evidence from one experiment at one location. However, the dominance of matrix flow observed from the Phase 1A test does not lose generality for the CHn vitric units. Support for this assessment is provided by the relatively high matrix permeability and porosity of the CHn vitric unit. Matrix permeabilities for CHn are usually a few orders of magnitude higher than welded tuffs (Table A-1) (BSC 2003c, Tables 3 and 4). In addition, the nonwelded vitric layers within the CHn units have a low degree of fracturing (Table A-1). Under such conditions, the fractures embedded in a high-permeability matrix no longer function as fast paths for fluid flow (as do those in welded tuffs). Thus it is very likely that the matrix flow forms the majority of the total flux in the CHn unit, and that fracture flow is only a minor contributor.



Source: BSC 2003d, Figure 6.13.2-2.

Figure A-8. Fluorescein Plume at 90 cm Mineback Face at Borehole 3

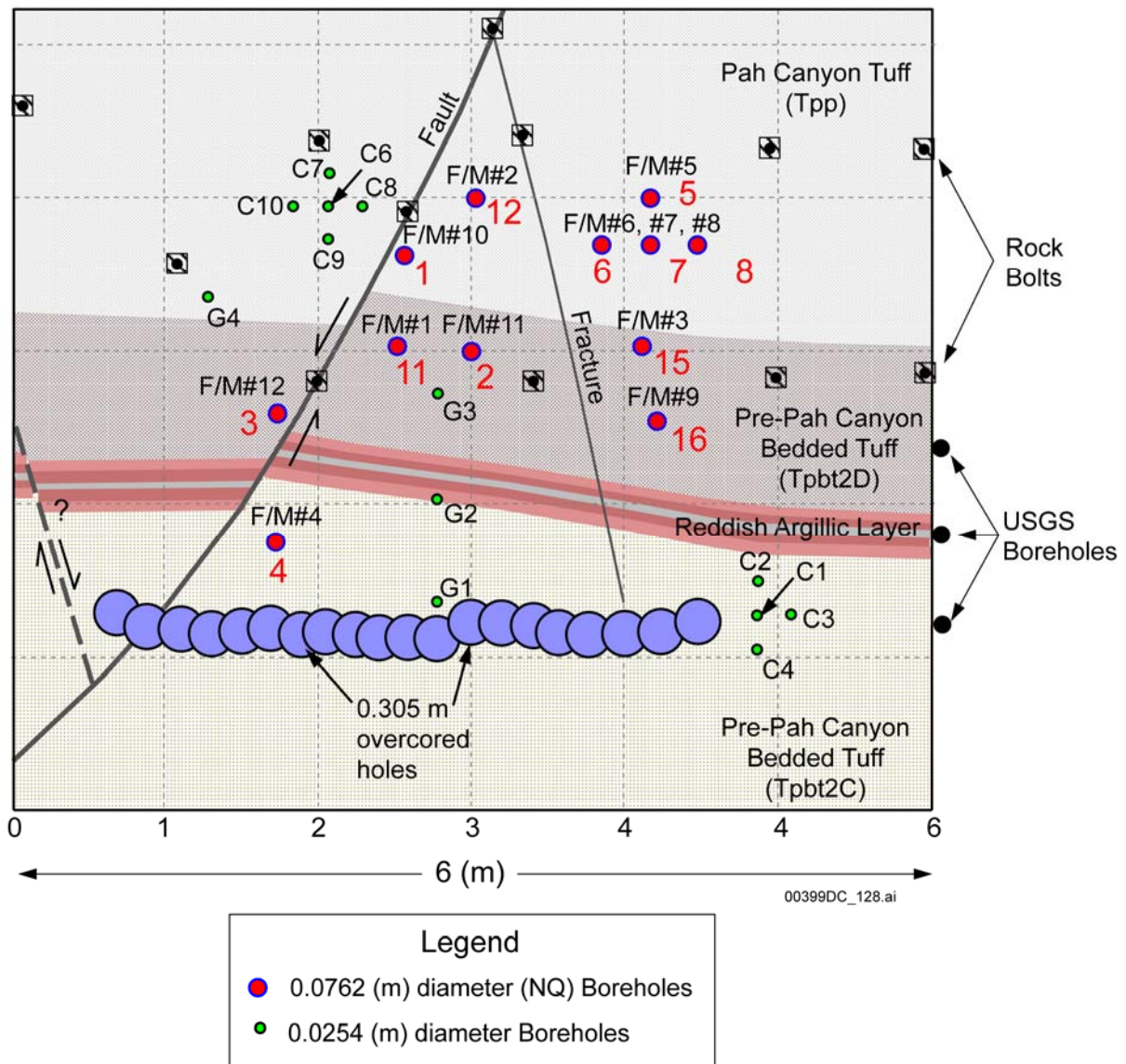
#### **A.4.4 Field Test at the Exploratory Studies Facility Alcove 4 in the PTn Unit**

As described in Section A.4.3, the effect of the fractures in the nonwelded vitric tuff layers at the CHn units can be considered negligible because of the relatively high matrix permeability (Table A-1). The insignificant role of fracture flow in the CHn vitric layers is corroborated by evidence from the ESF Alcove 4 experiment in the PTn unit, from which retarded flow and transport in a small fault have been observed. Alcove 4 is located in the ESF north ramp within the nonwelded tuffs of the PTn unit, which has low fracture densities, and relatively high matrix permeabilities and porosities (BSC 2003c, Tables 3 to 4, 11 to 13). Inside the PTn layers, Alcove 4 transects portions of the lower Pah Canyon Tuff (Tpp) and the upper pre-Pah Canyon bedded tuffs (Tpbt2) of the PTn (nomenclature of Buesch et al. 1996, p. 7). The test bed is located on the north face of the alcove, which is approximately 6 m wide and 5.3 m high (Figure A-9).

Exposed along the north face of Alcove 4 are the lower Tpp and upper Tpbt2 units D and C. Tpp is nonwelded and pumice-rich, exhibits a chalky-white color, and is apparently zeolitically altered. Tpbt2D is also nonwelded, possibly reworked, and has variably abundant (while zeolitically altered) pumice within a fine- to coarse-grained, medium-brown matrix. The contact between the lower Tpp and upper Tpbt2D is sharp in Alcove 4, marked by distinct color changes.

Below Tpbt2D, lying in the upper Tpbt2C, is a thin (0.20 to 0.30 m), light-pink to red argillically altered layer almost completely offset by a small, westward-dipping normal fault. The remaining Tpbt2C exposed along the north face below the argillic layer is massive and nonwelded, has very pale tan coloring, and contains abundant, coarse pumice and lithic fragments.

Cutting the north face of Alcove 4 is a normal fault with a small offset (0.25 m). As mapped along the crown at the end of the alcove, the fault has a strike of approximately 195° and a westward dip of 58°. The fault is open in the ceiling and is closed, with knife-edge thickness, near the invert on the north face. Intersecting the fault near the alcove crown along the north face is a high-angle fracture.

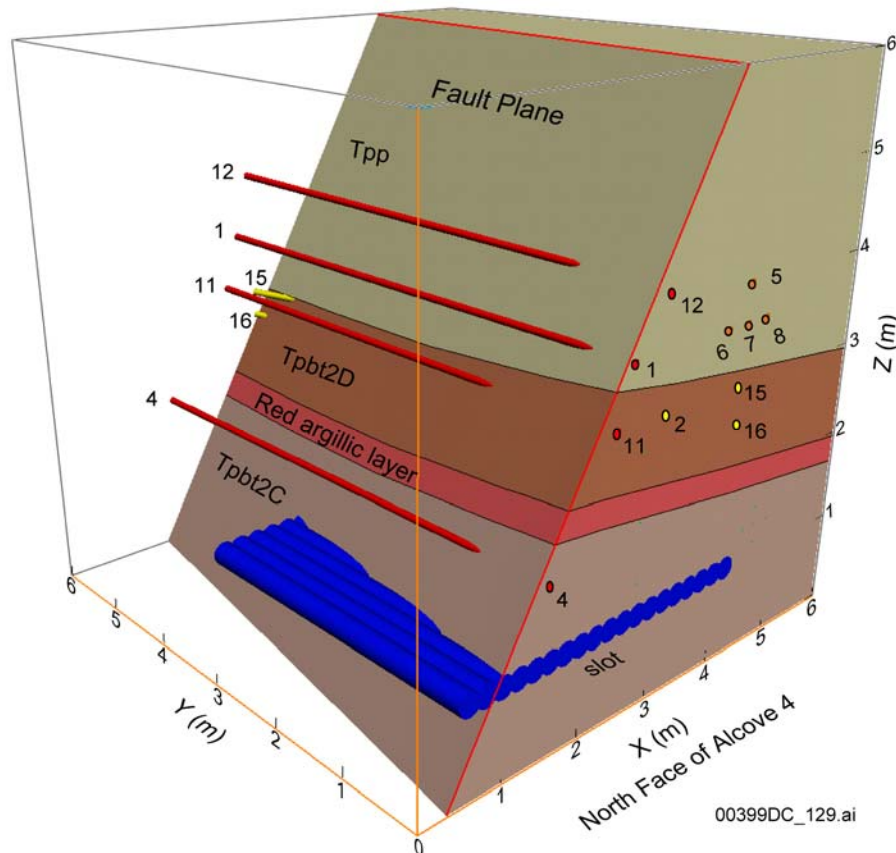


Source: BSC 2003d, Figure 6.7.1-1.

NOTE: Also included are the locations of boreholes and the slot. Boreholes labeled with red numbers were used in the field test of flow along the fault discussed in the text.

Figure A-9. Geologic Sketch and Schematic Illustration for the Test Bed in the North Face of Alcove 4 in the Exploratory Studies Facility

A total of twelve boreholes 6.0 m long and 0.0762 m wide were drilled into the alcove face, as illustrated in Figures A-9 (boreholes labeled with red) and A-10. Significantly, a number of boreholes (boreholes 1, 4, 11, and 12) were positioned to intersect the fault for the purpose of conducting flow tests within the fault. Borehole 2 was located to detect moisture that could migrate through the matrix below borehole 12. Borehole 12 was the injection borehole for the fault flow tests (BSC 2003d, Section 6.7.1.1). Liquid-release experiments were conducted at Alcove 4 and are described in detail in the document *In Situ Field Testing of Processes* (BSC 2003d, Section 6.7.1.1).



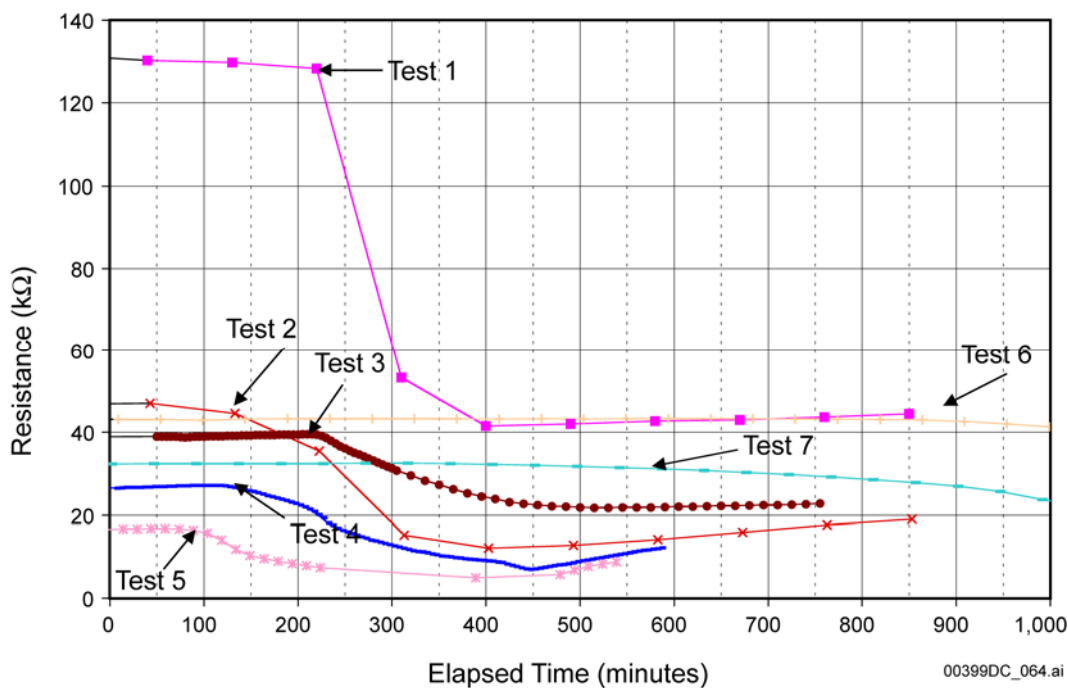
Source: BSC 2003d, Figure 6.7.1-2.

Figure A-10. Perspective Illustration of Three-Dimensional View of the Boreholes, Slot, and Lithologic Unit Contacts in the Alcove 4 Test Bed

In the liquid-release experiments, water was spiked with lithium bromide (BSC 2003d, Sections 6.5.2 and 6.7.1.3). The water was injected into the section of borehole 12 that intercepted the fault approximately 1.40 m from the collar. In this borehole, water was released over a 0.30 m interval. Here, the injection interval was centered at a distance 1.4 m from the borehole collar, determined from air-permeability measurements to be the location of the fault. A total of 193 L of water was released into the formation during seven events that extended over a period of two weeks, between October 21 and November 5, 1998. The time intervals between these tests (Tests 1-7) are approximately 1 day, with the exception of 4 days between Tests 2 and 3, and 7 days between Tests 5 and 6. Each event lasted between 4 and 7 hours, during which 20 to 43 L of water entered the injection zone. Each release event began with water filling the 1.37-L injection cavity in about 3 minutes, after which the liquid-release apparatus kept the injection zone filled by maintaining a constant-head boundary for the period of injection. After water was injected into the formation, the 1.37 L of water occupying the injection cavity was released to the formation under falling-head conditions.

The following examines the observed hydrological responses to liquid releases in borehole 12 as detected by electrical resistivity probes and psychrometers. Details of the tests regarding the intake rates are included the document *In Situ Field Testing of Processes* (BSC 2003d, Section 6.7.1.1).

The in-fault transport time was observed. When water was introduced into borehole 12, the time taken for the wetting front to travel 1.07 m along the fault to borehole 11 varied among the seven tests (Figure A-11). During the first release test, the wetting front advanced slowly, as a result of significant matrix imbibition. Specifically, water was detected in the lower borehole about 300 minutes after the first release, while in the second test, the travel time was reduced to about 200 minutes. For the third test, this travel time was about 250 minutes; in the fourth test, water appeared in the fault in borehole 11 within about 150 minutes. The fastest travel time was observed for the fifth test, when the wetting front arrived within about 120 minutes in borehole 11. In the last two tests, the travel times were significantly slower, with increasing saturations observed 400 and 700 minutes after the initial release of water.



Source: BSC 2003d, Figure 6.7.2-2.

Figure A-11. Wetting Front Arrival in Borehole 11 Following Liquid Released into the Fault in Borehole 12

It was observed that the wetting front during the first release test advanced slowly as a result of significant matrix imbibition. Given that water release rates used in the tests were much larger than water percolation rates under ambient conditions, the fracture flow in the PTn porous matrix is considered significantly dampened and leading to the dominance of matrix flow. The dry, porous PTn matrix is capable of attenuating episodic percolation fluxes in localized areas (such as around faults) where fast flow would otherwise be expected to dominate (Salve et al. 2003, p. 282). Test results show that fracture flow in the nonwelded tuffs is significantly retarded because of the matrix imbibition. The observation of retarded fault flow at the PTn unit provides a corroborative line of evidence for fracture flow in the nonwelded units including the vitric CHn.

#### **A.4.5 GEN 1.01 (Comment 26) Concerning the Multiple Interacting Continuum Model**

The multiple interacting continuum (MINC) model is more accurate than the dual permeability model in that it realistically reflects the transient fracture and matrix interaction. The model with MINC grid results in a later breakthrough time for a given concentration (BSC 2004, Figures 7 to 9, Section 7.2). This is because multiple interacting continua have higher spacing resolution in the matrix continuum enabling it to capture the transport of tracers (and radionuclides) from fracture into the matrix. However, the application of the MINC concept to the three-dimensional unsaturated zone site-scale model is overly burdensome for the incrementally greater accuracy because it necessitates replacement of the single matrix block in the current dual permeability system with several MINC subdomains. This increases the already large computation burden.

Considering all this, the present unsaturated zone flow model has adopted the dual-permeability approach for flow through both the fractures and the matrix (BSC 2003b, Section 6.1.2). Moreover, given that the dual permeability model yields earlier breakthrough times for a given concentration, the dual-permeability model can be considered more conservative than MINC model.

#### **A.4.6 Summary**

The nonwelded vitric layers within the bottom TSw unit and the CHn units have a low degree of fracturing and high porosity. The matrix permeabilities of the CHn vitric units are relatively high, usually approximately a few orders higher than welded tuffs (BSC 2003c, Tables 3 and 4). The fractures associated with the matrix of such high permeability no longer function as fast paths for fluid flow as do those in welded tuffs. This forms the basis of modeling the nonwelded vitric layers within the CHn units as single porosity matrix. This conceptualization of dominance of matrix flow in the vitric layers is supported directly by the Busted Butte field test and corroboratively by the Alcove 4 test.

Busted Butte provides rare exposure of vitric layers of the CHn units. Field testing at the vitric layers shows that a tracer coming across a fracture advanced without any alteration of its plume shape. This observation demonstrates that flow in the CHn occurs in the matrix only.

The reduced role of fractures in nonwelded tuffs was also observed in the nonwelded tuffs in the PTn unit. In comparison with vitric layers in the CHn, the PTn unit has lower matrix permeability and smaller fracture spacing. Flow testing along a small fault under initial dry condition within the PTn unit at the ESF Alcove 4 had a slowly advancing wetting front as a result of significant matrix imbibition, following the first liquid release test. Delay of the wetting front under ambient conditions is expected to be even more significant. This is because water percolation rates under ambient conditions are much smaller than water release rates under the test condition. This liquid release test at the fault within the PTn unit provides corroborative evidence regarding the diminished role of fractures in the nonwelded vitric tuffs of the CHn units.

The unsaturated zone flow model adopted the dual-continuum approach for flows through both the fractures and matrix (BSC 2003b, Section 6.1.2), producing relatively conservative results, as opposed to those from the MINC model.

## A.5 REFERENCES

- BSC (Bechtel SAIC Company) 2001. *FY01 Supplemental Science and Performance Analyses, Volume 1: Scientific Bases and Analyses*. TDR-MGR-MD-000007 REV 00 ICN 01. Las Vegas, Nevada: Bechtel SAIC Company. ACC: MOL.20010801.0404; MOL.20010712.0062; MOL.20010815.0001.
- BSC 2003a. *Radionuclide Transport Models Under Ambient Conditions*. MDL-NBS-HS-000008 REV 01. Las Vegas, Nevada: Bechtel SAIC Company. ACC: DOC.20031201.0002.
- BSC 2003b. *UZ Flow Models and Submodels*. MDL-NBS-HS-000006 REV01. Las Vegas, Nevada: Bechtel SAIC Company. ACC: DOC.20030818.0002.
- BSC 2003c. *Calibrated Properties Model*. MDL-NBS-HS 000003 REV 01. Las Vegas, Nevada: Bechtel SAIC Company. ACC: DOC.20030219.0001.
- BSC 2003d. *In Situ Field Testing of Processes*. ANL-NBS-HS-000005 REV 02. Las Vegas, Nevada: Bechtel SAIC Company. ACC: DOC.20031208.0001.
- BSC 2003e. *Development of Numerical Grids for UZ Flow and Transport Modeling*. ANL-NBS-HS-000015 REV 01. Las Vegas, Nevada: Bechtel SAIC Company. ACC: DOC.20030404.0005.
- BSC 2004. *Particle Tracking Model and Abstraction of Transport Processes*. MDL-NBS-HS-000020 REV 00. Las Vegas, Nevada: Bechtel SAIC Company. ACC: DOC.20040120.0001.
- Buesch, D.C.; Spengler, R.W.; Moyer, T.C.; and Geslin, J.K. 1996. *Proposed Stratigraphic Nomenclature and Macroscopic Identification of Lithostratigraphic Units of the Paintbrush Group Exposed at Yucca Mountain, Nevada*. Open-File Report 94-469. Denver, Colorado: U.S. Geological Survey. ACC: MOL.19970205.0061.
- Pruess, K. and Narasimhan, T.N. 1985. A Practical Method for Modeling Fluid and Heat Flow in Fractured Porous Media. *Society of Petroleum Engineers Journal*, 25, (1), 14-26. Dallas, Texas: Society of Petroleum Engineers. TIC: 221917.
- Reamer, C.W. and Gil, A.V. 2001. Summary Highlights of NRC/DOE Technical Exchange and Management Meeting of Range on Thermal Operating Temperatures, September 18-19, 2001. Washington, D.C.: U.S. Nuclear Regulatory Commission. ACC: MOL.20020107.0162.
- Reamer, C.W. and Williams, D.R. 2000. Summary of Highlights of NRC/DOE Technical Exchange and Management Meeting on Radionuclide Transport, December 5-7, 2000, Berkeley, California. Washington, D.C.: U.S. Nuclear Regulatory Commission. ACC: MOL.20010117.0063.
- Salve, R.; Oldenburg, C.M.; and Wang, J.S.Y. 2003. Fault-Matrix Interactions in Nonwelded Tuff of the Paintbrush Group at Yucca Mountain. *Journal of Contaminant Hydrology*, 62-63, 269-286. New York, New York: Elsevier. TIC: 254205.

INTENTIONALLY LEFT BLANK